BC Gru: a spot evolved shallow-contact binary in hierarchical triple system

Liao W.-P.[1,2,3,4], Qian S.-B.[5], Li P.[1,4], Li L.-J.[1,2,3], Fernández-Lajús Eduardo.[6,7], He J.-J.[1,2,3], Liu N.-P.[1,2,3], Zeng Q.-H.[1,4] and Fang X.-H.[8]

ABSTRACT

BC Gru is a southern triple system that contains spectral types of approximately K0, K0, and K components. To understand the physical and orbital properties of this special system and the evolution state, we conduct a study combining TESS and ground-based CASLEO observations. The discovery of variations in O'Connell effect could be explained by the evolution of cool and hot spots on the primary and secondary component, respectively. The $(O-C)$ curve shows a cyclical variation with a semi-amplitude of 0.016 days and a period of 58.37 yr. The cyclical change can be analyzed for the LTTE via the presence of third body that is orbiting around the central eclipsing binary in an eccentric orbit of $e_3 = 0.17$. It is suggested that the third body is probably a late K-type star. The orbital inclination is determined to be $i_3 \sim 30°$, which reveals that the third body is non-coplanar to the orbit of the central eclipsing binary. Further, we discovery that the variations of Max I and Max II coincide with the $(O-C)$ pattern of primary and secondary light minima during TESS observations, which

[1]Yunnan Observatories, Chinese Academy of Sciences (CAS), 650216 Kunming, P. R. China, liaowp@ynao.ac.cn

[2]Key Laboratory for the Structure and Evolution of Celestial Objects, Chinese Academy of Sciences, 650216 Kunming, P.R. China

[3]Center for Astronomical Mega-Science, Chinese Academy of Sciences, 20A Datun Road, Chaoyang District, Beijing, 100012, P. R. China

[4]University of Chinese Academy of Sciences, No.1 Yanqihu East Rd, Huairou District, Beijing, P.R.China 101408

[5]School of Physics and Astronomy, Yunnan University, Kunming 650091, China

[6]Facultad de Ciencias Astronómicas y Geofísicas, Universidad Nacional de La Plata, Paseo del Bosque S/N–B1900FWA, La Plata, Argentina

[7]Instituto de Astrofísica de La Plata (CCT La Plata–CONICET/UNLP), B1900FWA La Plata, Argentina

[8]School of Mathematics, Physics and Finance, Anhui Polytechnic University, Wuhu 241000, China

indicates that the very low amplitude variability of ~ 0.0006 day found in the $(O-C)$ curve is most likely caused by star spots.

Subject headings: stars: binaries (including multiple) : close – stars: binaries : eclipsing — stars: solar-type– stars: evolution – stars: individual (BC Gru)

1. Introduction

The formation and evolution of short period contact binaries (CBs) is not well understood. In a series of research on "contact binaries with additional components" (Pribulla & Rucinski 2006; D'Angelo et al. 2006; Rucinski et al. 2007, papers I–III, respectively), the authors suggest that CBs may have formed in triple or larger multiple systems, where the tertiary companions may facilitate or enable the formation of CBs via acquiring and/or absorbing angular momentum during the evolution of multiple systems, especially if the tertiary components were in an eccentric orbit.

BC Gru ($V = 10.74$ mag) was discovered by Hoffmeister (1963) in his photographic search for variable stars in southern star fields. Later it was included in the catalog of 63rd Name-list of variable stars (S 6498 [4001], Kholopov et al. 1978). Its photographic light curve and several eclipse times were published by Meinunger (1979). She derived also an early period of 0.26617 day and concluded that BC Gru is either a W UMa-type variable or an RRc-type variable. In the 4th Edition of General Catalogue of Variable Stars (GCVS) BC Gru is classified as EW:/KW: (Kholopov et al. 1985).

In the progress on the photometric study of short-period eclipsing binaries (Gomez et al. 1988), the V photoelectric partial light curve of BC Gru was obtained, showing a W UMa system with rather shallow eclipse, and an improved ephemeris was presented. The period of BC Gru was substantially modified to a longer value 0.3073070 ($\pm$0.0000098) day by them. Plewa & Kałużny (1992) revised the period to be 0.307356 ($\pm$0.000019) day from their multi-color photoelectric data. Their UVI light curves show only marginally asymmetric. The spectral type of G8V was suggested by them based on their color curves, and the primary component temperature was estimated to T_1 =5450 K. Simultaneous solutions of $BVRcIc$ light curves indicate that BC Gru is a rather shallow-contact ($f = 1.1\%$) binary with the mass ratio $q = 1.77$. Samec & Becker (1993) reported high precision multi-band light curves and four eclipse times, another improved ephemeris with a period of 0.30735687 (4) was given. Their very preliminary analysis showed that BC Gru is a very shallow-contact W-type binary with a difference temperature of $\Delta T \sim 400$ K and a large mass ratio of $q = 0.8$. Thereafter, those photometric information of BC Gru has been listed in several catalogs

or statistics study on W UMa stars (Pribulla et al. 2003; Avvakumova et al. 2013; Latković et al. 2021).

It was not until 2007 that the spectroscopic observations of BC Gru were developed by Dall et al. (2007) through the Variable Star One-shot Project (VSOP). The FEROS (Fibre-fed Extended Range Optical Spectrograph) spectrum confirmed the contact binary nature of BC Gru, meanwhile, revealed a third component. All three components have approximately the same spectral types of K0, K0, and K. They reported rotational velocities with large errors $(vsini)_a = 165 \pm 50$ km/s and $(vsini)_b = 142 \pm 50$ km/s for the binary, and $(vsini)_c = 6 \pm 3$ km/s for the tertiary component of the system. Ten years later, Moriarty (2016) published the first period analysis of BC Gru, the period was revised to 0.3073060(1) day. Moriarty commented that further time series observations are required to determine the effect of the third component in the system on the period of BC Gru. Moriarty's another aim was to develop a model solution based on detailed BVI_c asymmetry light curves obtained in 2014 and 2015 with a 356-mm Schmidt-Cassegrain telescope. He concluded that BC Gru is a W-subtype W UMa binary: $q_{ph} = 1.2$; $i = 69°$; $f = 8\%$; $l_{3B} = 9\%$, $l_{3V} = 12\%$, $l_{3I_c} = 19\%$, and the discovery that the $(O - C)$ diagram variation with a small modulations of 0.001 to 0.002 day in 2014 and 2015 is most likely caused by star spots. The third light contribution in I_c-band is the highest indicates that the third body should be a late K-type star.

Stellar atmospheric parameters of BC Gru can be accessed via the CDS VizieR service[1], where catalogs are mainly based on the RAVE DR6 that are cross-matched with relevant astrometric and photometric catalogs, and are complemented by orbital parameters and effective temperatures based on the infrared flux method (Shank et al. 2022; Steinmetz et al. 2020; Kunder et al. 2017; Kordopatis et al. 2013): $T_{eff} = 5050 \pm 120$ K, $\log g = 0.738$ cm/s^2, $[Fe/H] = -0.404 \pm 0.110$ dex.

As mentioned above, BC Gru has been observed by spectroscopy and photometry, a K-type third companion was revealed by the foregoing FEROS spectrum, a preliminary period analysis and photometric model solutions were reported, but a measurable light-travel-time effect (LTTE) in the orbital period changes and a modern light-curve solutions are lacking. We now have a good opportunity to further study the period changes and the evolution state of BC Gru by utilizing a longer time series of observations over several years, such as the 27-day continuous photometry data from the one of the most important ongoing all-sky projects Transiting Exoplanet Survey Satellite (TESS, Ricker et al. 2015) and the multi-band data observed at Complejo Astronomico El Leoncito (CASLEO, see Sec. 2). Simultaneously, the parallax of 5.2956 (8678) mas in Gaia EDR3 (Gaia Collaboration 2020) will make us

[1]https://vizier.cds.unistra.fr/viz-bin/VizieR-4

calculate the distance of binary. It is hoped that this joint study of ground-based and space photometric observations can help us understand the physical and orbital properties of this special triple system, the evolution of star spots on a short time scale, as well as analyse the correlation between the O'Connell effect (O'Connell 1951) and the high frequency, low amplitude variability in the $(O-C)$ diagram, etc.

2. New CCD observation and eclipse times accumulation

For this study, new photometric observations covering B, V, R_c, and I_c filters were performed for BC Gru during 11 nights from 2018 August to 2023 September. Our photometric observations were performed using two different telescopes at Complejo Astronomico El Leoncito (CASLEO, in Argentina): CASLEO 2.15 m and CASLEO 0.6 m. The detailed description of the adopted observational strategy and data reduction can be found in Agarwal et al. (2019). The phased observations for each night are displayed in Fig. 1 with different colors. Based on a series of eclipse light curves (hereafter LCs), a parabolic fitting method was used to determine eclipse times in different bands that are nearly the same as those determined with the Kwee & van Woerden (1956) method. Totally, 19 new eclipse times were obtained and are listed in Table 1.

In addition, TESS space mission can achieve continuous LCs of BC Gru. We downloaded the TESS LCs data from the service of the Mikulski Archive for Space Telescopes (MAST)[2], there are two sectors, tess-s0001(from BJD 2458325 to 2458353, about 27 days, with an exposure time of 2 minutes) and tess-s0028 (from BJD 2459061 to 2459087, about 25 days, with an interval of about 10 minute cadence). Finally, 327 eclipse times were determined by using the method mentioned by Shi et al. (2021), which are tabulated in Table 1, they are published in the machine-readable format. The sector for 2 minutes cadence (shown in the top of Fig. 2) together with the BVR_cI_c CASLEO LCs will be used to solve photometric model solutions and discuss the evolution of BC Gru system in Section 4. All the phased LCs after calculating with the equation of BJD = 2458325.37739 + 0.307306 × E are shown in the bottom of Fig. 2, where the color variation from dark blue to yellow represents changes over the time, and the Max I gets fainter and fainter, while the Max II has an opposite change.

[2]https://mast.stsci.edu/portal/Mashup/Clients/Mast/Portal.html

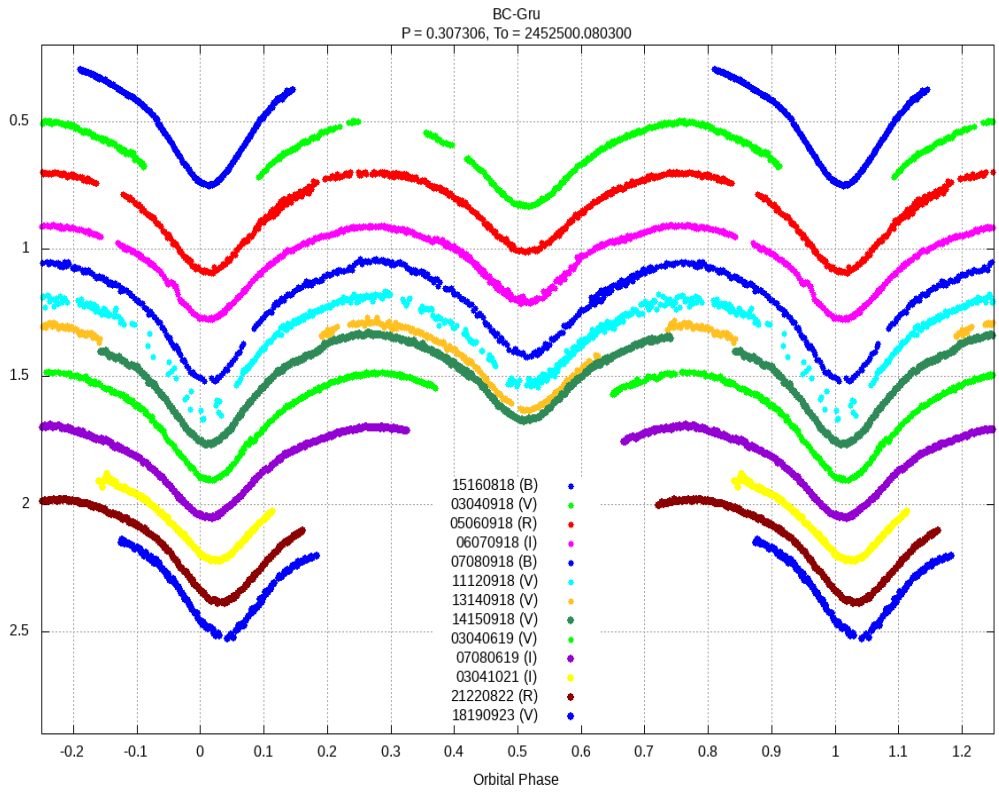

Fig. 1.— The phased eclipsing light curves observed at CASLEO, where different color lines represent different observational dates.

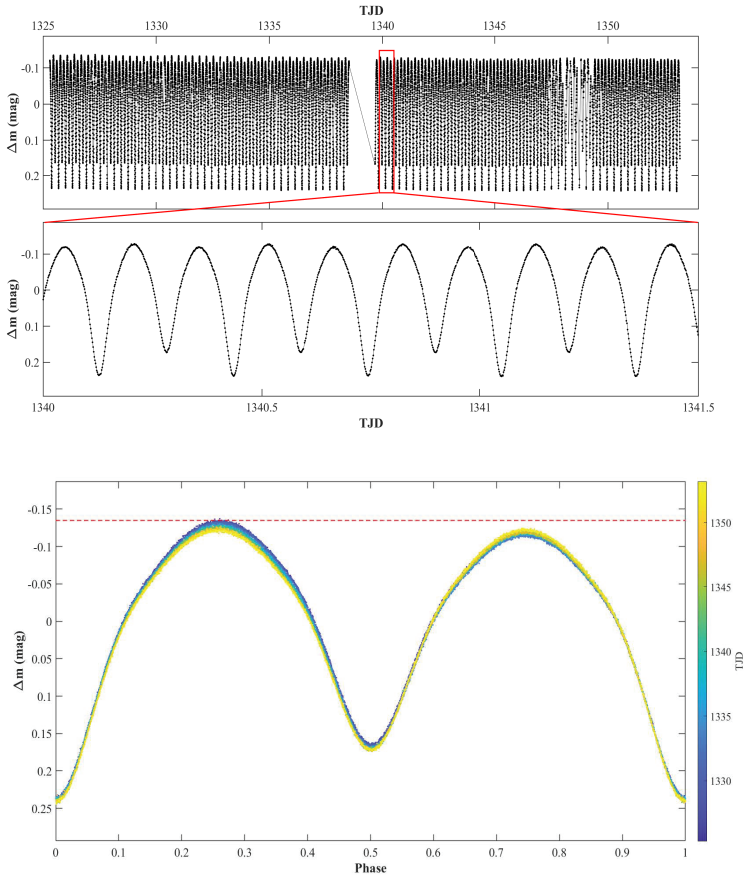

Fig. 2.— The TESS LCs of BC Gru with an interval of 2 minutes cadence (TJD = BJD-2457000.0), where the details of light curve for five cycles are also displayed in middle. Bottom panel: the phased TESS LCs, where the color variation from dark blue to yellow represents changes over the time.

Table 1: A total of 399 times of light minima for BC Gru. This is a sample of the full table, which is available in its entirety in machine-readable format.

Eclipse Times HJD-2400000	Error (± days)	Eclipse P/S	Source	Epoch	$O-C$ (days)	References
36814.292		P	Literature	-70089	0.0279	(1)
46686.65316	0.00007	S	Literature	-37963.5	0.0301	(2)
46686.80628	0.00027	P	Literature	-37963	0.0296	(2)
46687.72825	0.00019	P	Literature	-37960	0.0297	(2)
46688.80488	0.00019	S	Literature	-37956.5	0.0307	(2)
.....	.....	.....	.....	.....	.....	.....
58345.96621	0.00008	P	TESS	-23	-0.0001	(8)
58346.12009	0.00011	S	TESS	-22.5	0.0001	(8)
58346.27354	0.00010	P	TESS	-22	-0.0001	(8)
58346.42734	0.00010	S	TESS	-21.5	0.0001	(8)
58346.58081	0.00007	P	TESS	-21	-0.0001	(8)
58346.73459	0.00013	S	TESS	-20.5	0.0000	(8)
58346.88811	0.00008	P	TESS	-20	-0.0001	(8)
58346.88813	0.00003	P	CASLEO 2.15m	-20	-0.0001	(8)
58347.04186	0.00011	S	TESS	-19.5	0.0000	(8)
58347.19530	0.00009	P	TESS	-19	-0.0002	(8)
58347.35037	0.00070	S	TESS	-18.5	0.0012	(8)
58347.50263	0.00008	P	TESS	-18	-0.0002	(8)
.....	.....	.....	.....	.....	.....	.....
58365.78787	0.00007	S	CASLEO 0.6m	41.5	0.0003	(8)
58367.63189	0.00010	S	CASLEO 0.6m	47.5	0.0005	(8)
58367.78495	0.00008	P	CASLEO 0.6m	48	-0.0001	(8)
58368.55314	0.00015	S	CASLEO 0.6m	50.5	-0.0002	(8)
58368.70674	0.00008	P	CASLEO 0.6m	51	-0.0002	(8)
58368.86090	0.00021	S	CASLEO 0.6m	51.5	0.0003	(8)
58369.62887	0.00008	P	CASLEO 0.6m	54	0.0000	(8)
58369.78319	0.00014	S	CASLEO 0.6m	54.5	0.0007	(8)
58373.62315	0.00045	P	CASLEO 0.6m	67	-0.0007	(8)
58373.77863	0.00020	S	CASLEO 0.6m	67.5	0.0011	(8)
58375.62187	0.00009	S	CASLEO 0.6m	73.5	0.0005	(8)
58376.54342	0.00008	S	CASLEO 0.6m	76.5	0.0002	(8)
58376.69716	0.00005	P	CASLEO 0.6m	77	0.0002	(8)
58638.82994	0.00007	P	CASLEO 0.6m	930	0.0010	(8)
58642.82426	0.00007	P	CASLEO 0.6m	943	0.0004	(8)
.....	.....	.....	.....	.....	.....	.....
59085.80779	0.00052	S	TESS	2384.5	0.0023	(8)
59085.96023	0.00077	P	TESS	2385	0.0011	(8)
59086.11482	0.00043	S	TESS	2385.5	0.0020	(8)
59086.26837	0.00084	P	TESS	2386	0.0019	(8)
59086.42194	0.00049	S	TESS	2386.5	0.0018	(8)
59086.57526	0.00062	P	TESS	2387	0.0015	(8)
59086.72977	0.00055	S	TESS	2387.5	0.0023	(8)
59086.88274	0.00083	P	TESS	2388	0.0017	(8)
59491.60682	0.00007	P	CASLEO 0.6m	3705	0.0037	(8)
59813.66589	0.00006	P	CASLEO 0.6m	4753	0.0061	(8)
60206.71151	0.00012	P	CASLEO 0.6m	6032	0.0074	(8)

References: (1)Paschke, A. (2010); (2) Plewa & Kaluzny (1992); (3) Gomez et al. (1988); (4) Samec & Becker (1993); (5) Pribulla et al. (2003); (6) Moriarty (2016); (7) Juryšek et al. (2017); (8) This paper.

3. Period variation analysis

Dall et al. (2007) reported that BC Gru is a triple system with same spectral types of about K0, K0, and K components. The rotational velocities for three components of the system were given with large errors by them. However, the physical and orbital characteristics of the third body have not been studied since then. Moriarty (2016) reported a simple continuous period increase pattern of BC Gru and revised the period of the binary system as 0.307306 day. As Moriarty (2016) pointed out, further time series of observations are required to determine the effect of the third body on period variations of the BC Gru, and to determine the influence of other causes of period changes. We totally collected 399 eclipse times for BC Gru, including 53 ones from literature, 327 new TESS eclipse times and 19 ones from our CCD observations at CASLEO. All eclipse times are listed in the first Column of Table 1. Those shown in the Column 2 are errors of eclipse times, in the Columns 3-4 are eclipse types and sources of data, in the Column 7 are references of data. A detailed and improved analysis of period variations for the BC Gru system are given in this study. Expect to find a measurable LTTE in the orbital period analysis, and study the physical and orbital characteristics of the tertiary companion.

The epoch numbers and $(O-C)$ values were calculated with the following linear ephemeris, where T_0 is one of our new eclipse times,

$$MinI = 2458353.03435 + 0^{\rm d}.307306 \times E. \quad (1)$$

The epoch numbers and $(O-C)$ values are listed in the Columns 5-6 of Table 1 and plotted in the upper panel of Fig. 3. In the analysis of the $(O-C)$ diagram, an eccentric orbit of the tertiary component rotating around the central binary was considered. The trend of variations in $(O-C)$ curve was fitted with the following general equation (Irwin 1952),

$$\begin{aligned} O-C &= \Delta T_0 + \Delta P_0 E + \frac{\beta}{2}E^2 + A[(1-e_3^2)\frac{\sin(\nu+\omega)}{1+e_3\cos\nu} \\ &\quad +e\sin\omega] \\ &= \Delta T_0 + \Delta P_0 E + \frac{\beta}{2}E^2 \\ &\quad +A[\sqrt{1-e_3^2}\sin E^*\cos\omega + \cos E^*\sin\omega] \end{aligned} \quad (2)$$

and the Kepler equation:

$$M = E^* - e_3\sin E^* = \frac{2\pi}{P_3}(t-T_3), \quad (3)$$

where the meaning of each parameter is described in a recent paper of Liao et al. (2021).

Due to the low reliability of parabolic plus cyclical variation fitting, we tried to analyze the $(O-C)$ diagram without parabolic variation (i.e., $\beta = 0$). Its fitting results are shown in the upper panel of Fig. 3. The residuals of fitting are shown in the lower panel of Fig. 3. The $(O-C)_1$ diagram in the middle panel shows an apparent cyclic oscillation with a semi-amplitude of 0.016 day and a period of 58.37 yr. The corresponding fitted parameters are listed in Table 2.

In addition to the overall trend of changes mentioned above, we discover an obvious high frequency variability ($\sim$ 0.05 yr) with a very small modulation of 0.0006 day during TESS observations (shown in the top panel of Fig. 4), which is most likely caused by star spots (Kalimeris et al. 2002; Moriarty 2016). To study the correlation between the effect of star spots and such high frequency, low amplitude variability in the $(O-C)$ diagram during TESS observations, and to study the variation of LCs, the variations of the corresponding Max I and Max II from all the LCs are plotted in the middle and bottom panels of the Fig. 4. The middle panel shows the variations of Max I and Max II. The bottom panel presents the variations of the Max I - Max II, where the Max I - Max II between TJD 1325 - TJD 1345 are not close to zero, thus, we try to divide all of those asymmetrical LCs in this interval into three parts to analyse the spot evolution in Section 4: Part A (TJD 1325-1330), Part B (TJD 1333-1338) and Part C (TJD 1339-1344), separated by red and magenta dash lines. As one can see from Fig. 4, the variations of Max I and Max II coincide with the $(O-C)$ curves of the primary and secondary minima during TESS observations.

4. Modern light-curve solutions

We selected a set of symmetric CASLEO BVR_cI_c LCs ($20180907B$; $20180913,14V$; $20180905R_c$; $20180906I_c$) from the Fig. 1 to solve basic light-curve solutions without spots. Seen from the lower panel of the Fig. 4, the continuous TESS light-curves from TJD 1325 to TJD 1345 exhibit an asymmetric and noticeable positive O'Connell effect, where the first light maximum at phase 0.25 (Max I) is brighter than the second maximum at phase 0.75 (Max II). It is a common and complex phenomenon in eclipsing binaries that Max I and Max II are not equal in height. Any mode that can cause local brightness change of the surface of the binary components, such as spots, mass transfer and so on, could cause this phenomenon (Shi et al. 2021; Liao et al. 2022). Those three asymmetric TESS LCs, i.e., Parts A, B and C, could provide a good opportunity to study the star spot's continuous evolution on short-time scales.

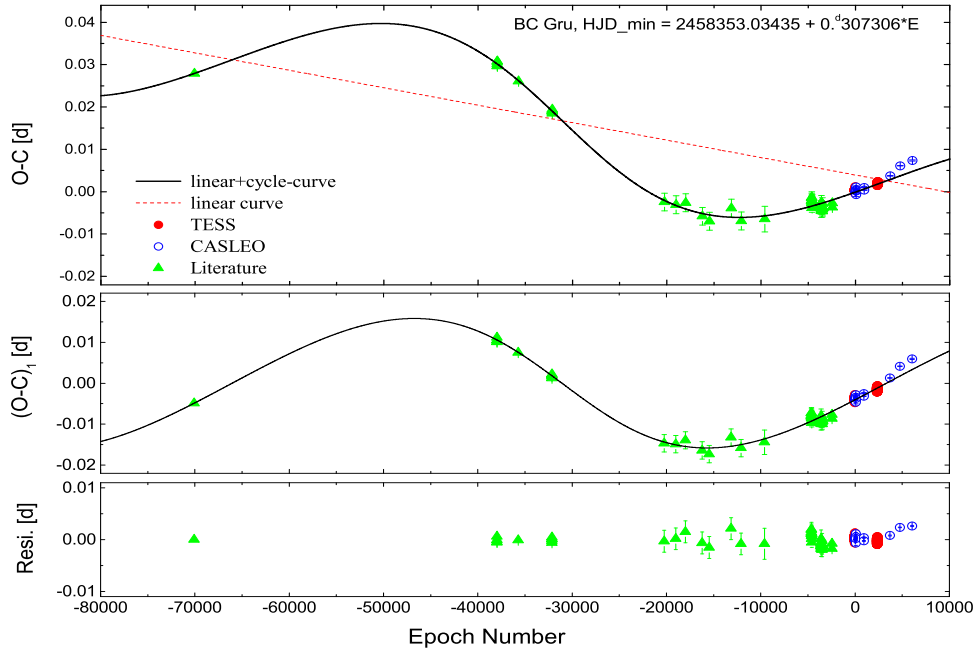

Fig. 3.— The $(O-C)$ diagrams of BC Gru fitted with an eccentric orbit for the pattern of linear plus cyclical fit. The data sources and colored lines are noted in the upper panel, the cyclical variations alone are shown in the middle panel, and the residuals from the whole effect are displayed in the bottom panel.

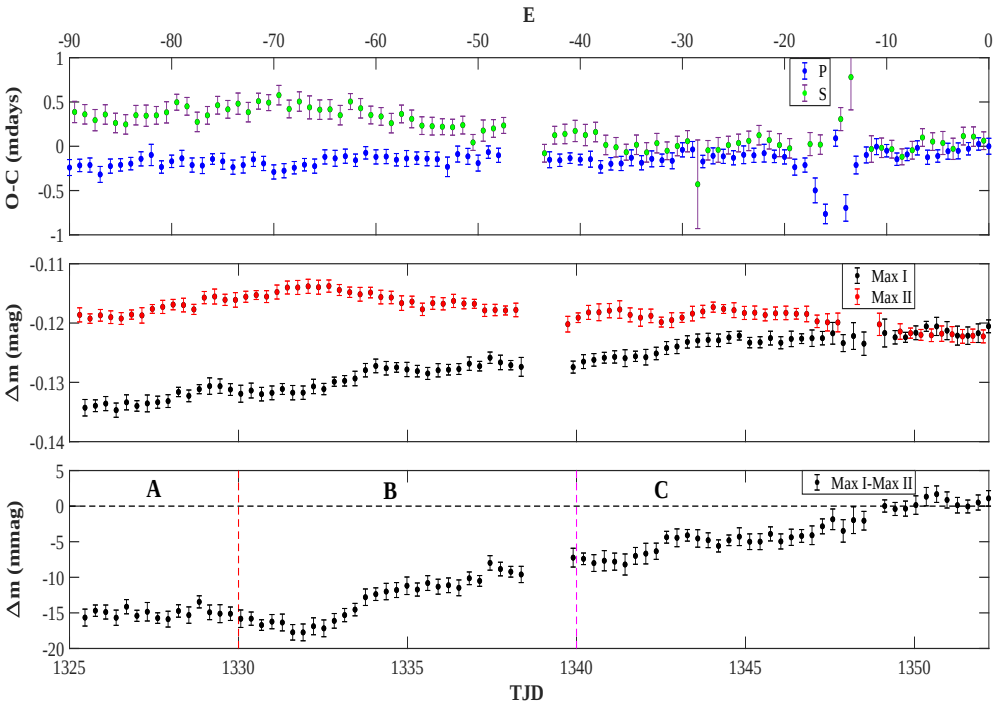

Fig. 4.— The variation trends of the $(O-C)$ curves during TESS observation, the Max I, the Max II, and the Max I - Max II. Top panel: the variations of the $(O-C)$ curves during TESS observation. Middle panel: the variations of the Max I and the Max II. Bottom panel: the variations of the Max I - Max II, where the variations during TJD 1325 - TJD 1345 can be divided into three parts A, B and C separated by red and magenta dash lines.

Table 2: Orbital parameters of the third body in the BC Gru system.

Parameters	Linear + cyclical variation
Revised epoch, ΔT_0 (days)	0.0039($\pm$0.0035)
Revised period, ΔP_0 (days)	$-4.12(\pm1.21) \times 10^{-7}$
Semi-amplitude, A (days)	0.0160 ($\pm$0.0019)
Orbital period, P_3 (yrs)	58.37 ($\pm$6.04)
Rate of the period change, $\dot{P}$ (day yr^{-1})	0 (assumed)
Longitude of the periastron passage, ω (deg)	184.46 ($\pm$9.60)
Time of periastron passage, T_3 (HJD)	2449025.03 ($\pm$0.06)
Eccentricity, e_3	0.17 ($\pm$0.08)
Projected semi-major axis, $a_{12}\sin i_3$ (au)	2.77 ($\pm$0.33)
Mass function, $f(m)$ ($M_\odot$)	0.0063 ($\pm$0.0022)
Mass, M_{3min} ($M_\odot$)	0.27 ($\pm$0.04)
Orbital semi-major axis, a_{3max} (au)	15.43 ($\pm$2.74)
The case of late K9-type tertiary companion:	
Mass, M_3 ($M_\odot$)	0.59 (assumed)
Orbital inclination, i_3 (deg)	30
Orbital semi-major axis, a_3 (au)	13.74 ($\pm$2.60)
Projected semi-major axis, a_{12} (au)	5.54 ($\pm$0.66)

All LCs are analyzed by using 2015 Wilson–Devinney (W–D) code (Van Hamme & Wilson 2007; Wilson 2012 and Wilson & Devinney 1971). According to the spectral type K0 for the primary star (Star 1), its temperature is fixed to be 5240 K (Cox 2000), thus its gravity-darkening and bolometric albedos coefficients are set to $g_{1,2} = 0.32$ and $A_{1,2} = 0.5$. The bolometric and bandpass limb-darkening coefficients were obtained by using an internal computation with the logarithmic law.

To check the mass ratio values, a series of trial values of q were assumed , i.e., a common technique called q-search method. The resulting mean residuals $\overline{\Sigma}$ for each q are plotted in left panel of Fig. 5. As seen from this panel, the minimum value of $\overline{\Sigma}$ is achieved at $q = 0.66$. Because the fact that the K-type tertiary in the system could contribute light to the total system, we decided to calculate a photometric solution with a third light. Therefore, in the process of fitting, we expanded the free parameters beyond just the mass ratio q, including the orbital inclination i; the effective surface temperature of secondary T_2; the monochromatic luminosity of primary L_1; the modified dimensionless surface potential ($\Omega_1 = \Omega_2$ for contact configuration Model 3); and the third light l_3. Iterations were performed with the initial input parameters of $q = 0.66$ until convergence. The final solutions were derived and listed in Table 3 for symmetrical CASLEO LCs. The diagram of without-spot fitting for CASLEO is shown in the right panel of Fig. 5. The observational LCs (the black circles), the theoretical fitting LCs (the solid colored lines), and the theoretical geometrical structures are displayed.

For the asymmetric TESS LCs, we expanded the spot parameters as adjustable parameters (see notes in Fig. 6 for details) beyond above free parameters. The final spots-fitting solutions for three sets of asymmetric TESS LCs were derived. The theoretical LCs described with a cool spot on the primary component and a hot spot on the secondary component plus a third light were displayed as red solid lines in the Fig. 6, in which the spots parameters and the theoretical geometrical structures for TESS are also listed. The two spots are evolving over a short-time scale and their positions are roughly symmetrical with the inner Lagrange L1 point. The contribution of the third light in TESS-band is even higher, at about 20 %.

5. Discussions and Conclusions

By using a longer time series of observations over several years, i.e., the continuous photometry data from TESS and the data observed at CASLEO, a photometric study of space and ground-based observations for the special triple system BC Gru that contains spectral types of about K0, K0, and K components was given in present paper. The orbital period variations are re-analyzed in detail by using a total of 399 eclipse times. It is discovered that the $(O-C)$ curve of BC Gru shows a pattern of "linear + cyclical variation" with a semi-

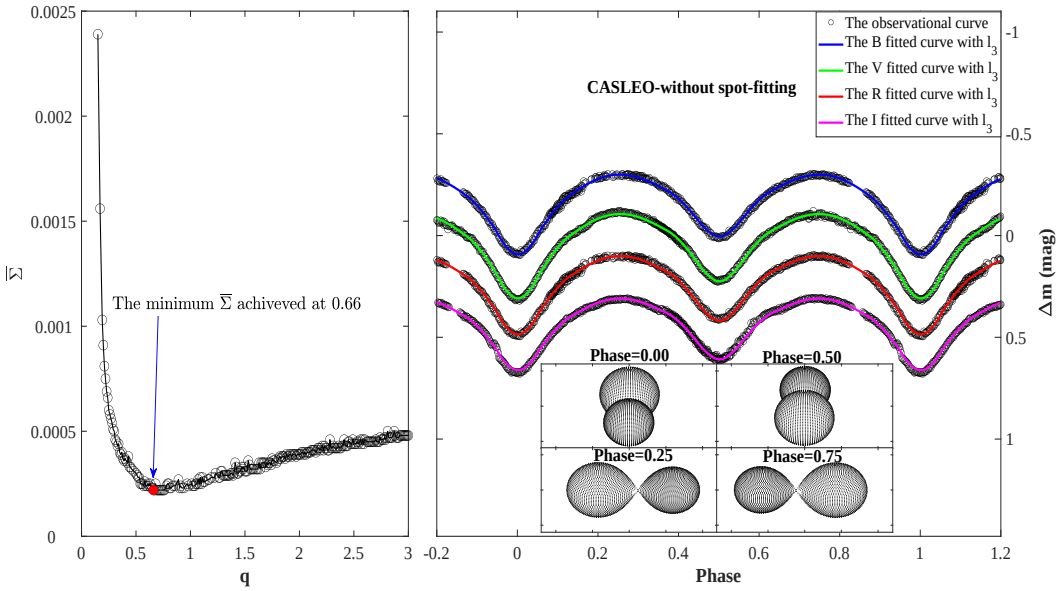

Fig. 5.— The diagram of without-spot fitting obtained using the W-D program. Left panel: the relation between q and $\overline{\Sigma}$ determined by model 3. Right panel: the CASLEO multi-band observation light curves (the black circles), the theoretical fitting light curves (the solid colored lines), and the theoretical geometrical structures.

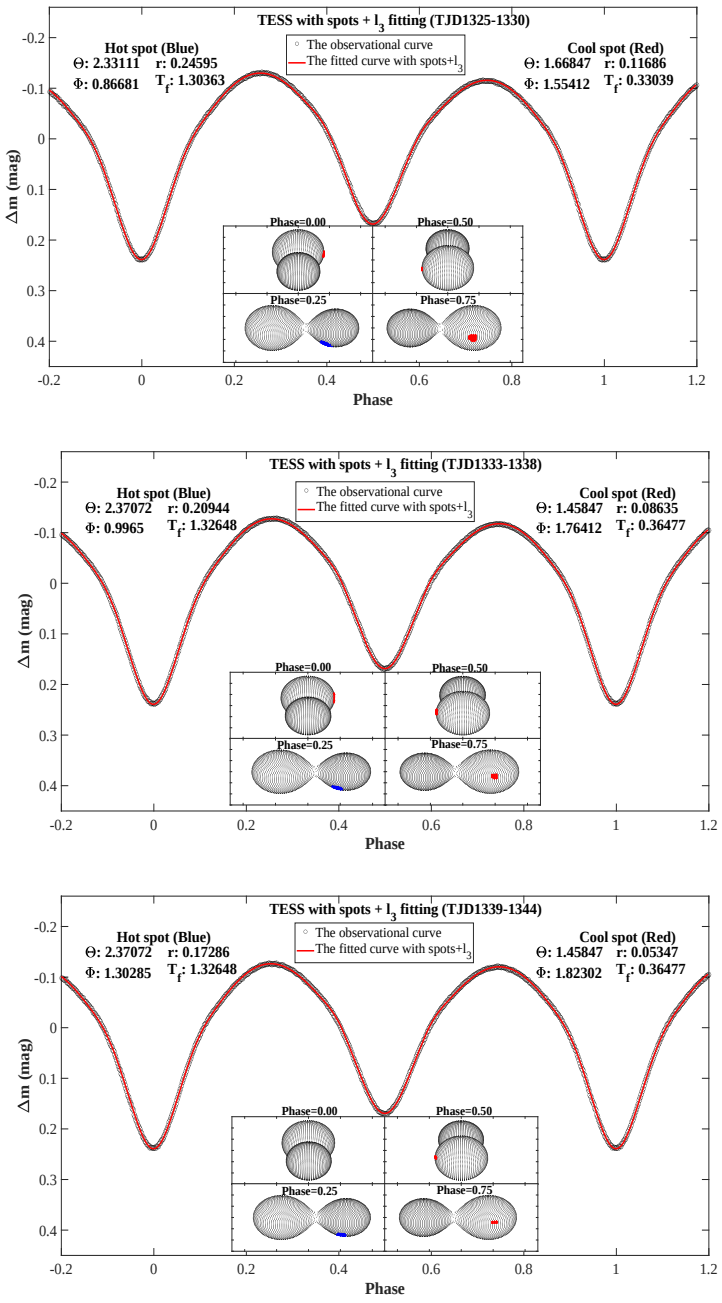

Fig. 6.— TESS spotted fitting. The three TESS asymmetric light curves corresponding to A-B-C (i.e., TJD 1325-1330, TJD 1333-1338, TJD 1339-1344) can be fitted well with an evolving hot spot (blue spot) on the secondary star and an evolving cool spot (red spot) on the primary star. Their positions are roughly symmetrical with the inner Lagrange L1 point. Spot parameters are written in the diagram: the latitude of a star spot center (Θ, in radian), the longitude of a star spot center (Φ, in radian), the radius of a star spot (r, in radian), the temperature factor of a spot (T_f, the ratio of the local spot temperature to the local temperature which would be obtained without the spot).

Table 3: Photometric solutions of BC Gru using the W–D code. The errors are expressed in parenthesis, in units of last decimal places quoted.

Parameter	CASLEO symmetrical LCs
T_1 (K)	5240 (fixed)
$i(^\circ)$	67.10(12)
q (M_2/M_1)	0.71034(60)
T_2/T_1	0.94046(65)
$\Omega_1 = \Omega_2$	3.25878(12)
$L_1/(L_1+L_2)_B$	0.6823(14)
$L_1/(L_1+L_2)_V$	0.6622(14)
$L_1/(L_1+L_2)_{R_c}$	0.6473(15)
$L_1/(L_1+L_2)_{I_c}$	0.6370(16)
$L_3/(L_1+L_2+L_3)_B$	0.0943(54)
$L_3/(L_1+L_2+L_3)_V$	0.0010(66)
$L_3/(L_1+L_2+L_3)_{R_c}$	0.0304(64)
$L_3/(L_1+L_2+L_3)_{I_c}$	0.0755(61)
r_1(pole)	0.385229(81)
r_1(side)	0.40662(11)
r_1(back)	0.43644(18)
r_2(pole)	0.32830(12)
r_2(side)	0.34364(15)
r_2(back)	0.37576(26)
f (%)	0.6(3)
r_1	0.410866(72)
r_2	0.35069(10)
R_2/R_1	0.85354(30)
Mean residual	0.0016

amplitude of 0.0160 (±0.0019) days and a period of 58.37 (±6.04) yr. The cyclical change in the $(O-C)$ diagram can be analyzed for the LTTE via the potential of a third body in an eccentric orbit. Furthermore, during TESS observations, an obvious high frequency variability ($\sim$ 0.05 yr) with a very small modulation of $\sim$ 0.0006 day in the $(O-C)$ curve was also indicated. We discovered that the variations of Max I and Max II coincide with the $(O-C)$ curve of the primary and secondary light minima during TESS observations, which indicates that this very low amplitude variability is most likely caused by star spots (Kalimeris et al. 2002; Moriarty 2016).

According to the Table 5 of Pecaut & Mamajek (2013) and K0-type for primary component, its mass was set as $M_1 = 0.88$ $M_\odot$, the mass of secondary component was then calculated to be $M_2 = 0.62$ $M_\odot$ ($q_{ph} = 0.71$). Using the commonly used mass function equation of multiple system (Liao et al. 2019, 2021, 2022) and the masses of binary components, the orbital parameters of the third body in BC Gru system were derived and listed in the Table 2. The minimum mass of the third body was estimated to be $M_{3min} = 0.27\,(\pm0.04)$ $M_\odot$, and the maximum orbital semi-major axis was 15.43 (±2.74) au. The third body is orbiting the central eclipsing binary in an eccentric orbit ($e_3 = 0.17\,(\pm0.08)$). From the FEROS spectrum of BC Gru in Fig. 2 given by Dall et al. (2007), it can be preliminarily inferred that the third component should be a late K-type star. Additionally, both the result of small third light contribution and the contribution in red band direction is higher (Moriarty, 2016; the present paper) suggest that the third body is probably a late-type star. If it is a single main-sequence star, it is most likely a K9 type star. Then the orbital parameters of such tertiary companion would be derived and listed in the lower part of Table 2. The orbital inclination is determined to be $i_3 \sim 30°$, which reveals that the third body is non-coplanar to the orbit of the central eclipsing binary. By using the orbital separation of the tertiary $d_3 = a_{12} + a_3 = 19.28$ au and the orbital period of $P_3 = 58.37$ years, the expected mean velocity of the third body can be easily estimated to be 9.84 km s^{-1} ($V_3 = 2\pi d_3/P_3$, assuming the third body moves in an approximately circular orbit around eclipsing pair). Using the parallax value of the Gaia EDR3, the Gaia distance of BC Gru is calculated to be 188.84 (±30.94) pc. Thus, the angular separation between the tertiary and the central eclipsing binary is then determined to be small $0''.10$.

The present photometric solutions suggest that BC Gru is a spot evolved shallow-contact binary. The short-time scale variations in O'Connell effect could be caused by the evolution of a cool spot on the primary component and a hot spot on the secondary component. It is found that their positions are roughly symmetrical with the inner Lagrange L1 point, which is like that in some analyses (e.g., Shi et al. 2021, Li et al. 2023). All of our results indicate that BC Gru is a shallow-contact binary with spots evolution in a hierarchical triple system. The tertiary companion in an eccentric and non-coplanar orbit has an important

role in the formation of BC Gru via acquiring and/or absorbing angular momentum during the evolution of multiple systems.

This work is supported by the National Natural Science Foundation of China (No. 11933008), the Young Talent Project of "Yunnan Revitalization Talent Support Program" in Yunnan Province, the basic research project of Yunnan Province (Grant No. 202201AT070092), CAS "Light of West China" Program and the Natural Science Foundation of Anhui Province (2208085QA23). We acknowledge with sincerest thanks the CASLEO telescope allocation committee and staff members and night assistants of CASLEO for their support.

The TESS data presented in this paper were obtained from the Mikulski Archive for Space Telescopes (MAST) at the Space Telescope Science Institute (STScI). STScI is operated by the Association of Universities for Research in Astronomy, Inc. Support to MAST for these data is provided by the NASA Office of Space Science. Funding for the TESS mission is provided by the NASA Explorer Program.

This work makes use of data from the European Space Agency (ESA) mission Gaia (https://www.cosmos.esa.int/gaia), processed by the Gaia Data Processing and Analysis Consortium (DPAC, https://www.cosmos.esa.int/web/gaia/dpac /consortium). Funding for the DPAC has been provided by national institutions, in particular the institutions participating in the Gaia Multilateral Agreement.

REFERENCES

Agarwal, A.; Cellone, S. A.; Andruchow, I.; Mammana, L.; Singh, M.; et al., 2019, MNRAS, 488, 4093

Avvakumova, E. A.; Malkov, O. Y.; & Kniazev, A. Y. 2013, AN, 334, 860

Cox, A. N. 2000, Allen's Astrophysical Quantities (New York: AIP)

Dall, T. H.; Foellmi, C.; Pritchard, J.; Lo Curto, G.; Allende Prieto, C.; et al., 2007, A&A, 470, 1202

D'Angelo, C.; van Kerkwijk, M. H.; & Rucinski, S. M. 2006, AJ, 132, 650

Gaia Collaboration 2020, yCat, I/350

Gomez, M.; Lapasset, E.; Ahumada, J.; Clariá, J. J.; & Minniti, D. 1988, BAAA, 34, 119

Hoffmeister, C. 1963, Veroff. Sternwarte Sonnenberg, 6, 1

Irwin, J. B. 1952, ApJ, 116, 211

Juryšek, J.; Hoňková, K.; Šmelcer, L.; Mašek, M.; Lehký, M.; et al., 2017, OEJV, 179, 1

Kalimeris, A.; Rovithis-L. H.; & Rovithis, P. 2002, A&A, 387, 969

Kholopov, P. N.; Kukarkina, N. P.; & Perova, N. B. 1978, IBVS, 1414, 1K

Kholopov, P. N.; Samus, N. N.; Kazarovets, E. V.; & Perova, N. B. 1985, IBVS, 2681, 1

Kordopatis, G.; Gilmore, G.; Steinmetz, M.; Boeche, C.; Seabroke, G. M.; et al., 2013, AJ, 146, 134

Kunder, A.; Kordopatis, G.; Steinmetz, M.; Zwitter, T.; McMillan, P. J.; et al., 2017, AJ, 153, 75

Kwee, K. K., & van Woerden, H. 1956, BAN, 12, 327

Latković, O.; Čeki, A.; & Lazarević, S. 2021, ApJS, 254, 10

Li, P.; Liao, W. P.; Qian, S. B.; Li, L. J.; Fang, X. H.; et al. 2023, under review

Liao, W. P.; Qian, S. B.; & Li, L. J. 2021, MNRAS, 508, 6111

Liao, W. P.; Qian, S. B.; & Sarotsakulchai, T. 2019, AJ, 157, 207

Liao, W. -P.; Qian, S. -B.; Shi, X. -D.; Li, L. -J.; Liu, N. -P.; et al., 2022, ApJ, 927, 183

Meinunger, I. 1979, VeSon, 9, 105

Moriarty, D. J. W. 2016, JAVSO, 44, 10

O'Connell, D. J. K. 1951, PRCO, 2, 85

Paschke, A. 2010, OEJV, 130, 1

Pecaut, M. J.; & Mamajek, E. E. 2013, ApJS, 208, 9

Plewa, T.; & Kałużny, J. 1992, AcA, 42, 103

Pribulla, T.; Kreiner, J. M.; & Tremko, J. 2003, CoSka, 33, 38

Pribulla, T.; & Rucinski, S. M. 2006, AJ, 131, 2986

Ricker, G. R.; Winn, J. N.; Vanderspek, R.; Latham, D. W.; Bakos, G. Á.; et al., 2015, JATIS, 1, 014003

Rucinski, S. M.; Pribulla, T.; & van Kerkwijk, M. H. 2007, AJ, 134, 2353

Samec, R. G.; & Becker, K. 1993, IBVS, 3891, 1

Shank, D.; Komater, D.; Beers, T. C.; Placco, V. M.; & Huang, Y. 2022, ApJS, 261, 19

Shi, X. D.; Qian, S. B.; Li, L. J.; & Liao, W. P. 2021, MNRAS, 505, 6166

Shi, X. D.; Qian, S. B.; Li, L. J.; & Liu, N. P. 2021, AJ, 161, 46

Steinmetz, M.; Guiglion, G.; McMillan, P. J.; Matijevič, G.; Enke, H.; et al., 2020, AJ, 160, 83

Van Hamme, W.; & Wilson, R. E. 2007, ApJ, 661, 1129

Wilson, R. E. 2012, AJ, 144, 73

Wilson, R. E., & Devinney, E. J. 1971, ApJ, 166, 605